The μZ-CGRS

Continuous Geodetic Reference System

June 2001

Magellan Corporation
Ashtech Precision Products
471 El Camino Real
Santa Clara, CA 95050
www.ashtech.com
408-615-5100 - main
800-229-2400 - support

1. INTRODUCTION

Ashtech Reference Stations are regarded worldwide as the leading choice for continuously operating GPS and GNSS reference receivers. They are found in the most demanding applications, including the US National Differential GPS system, the Southern California Integrated GPS Network, Japan's Geographical Survey Institute Network, the International GPS Service (IGS), The US National Geodetic Survey CORS network, and the United States Geological Survey site at the South Pole.

The Ashtech Micro Z Continuous Geodetic Reference Station (µZ-CGRS) System provides the world's most powerful GPS Reference Station technology at an affordable price. At the heart of the µZ-CGRS system is the new Ashtech µZ-CGRS GPS receiver. The µZ-CGRS is the latest and most advanced receiver in the Z family, and it incorporates patented Z-Tracking, the proven best technique for recovering the GPS carrier phase when Anti-Spoofing (A-S) is activated. Designed for high-accuracy scientific, engineering, land survey, and GIS reference applications, the µZ CGRS system is ideal as a permanent GPS base station.

2. PRODUCT FEATURES AND CONFIGURATIONS

.

Figure 1. µZ-CGRS Receiver and Choke Ring Antenna

The µZ-CGRS Receiver comes as a complete package ready to install. The receiver is available with an IGS-type choke ring antenna (figure 1). Geodetic patch antennas are also available.

Front Panel

Three LEDs on the front panel show the status of different activities within the receiver (figure 1). The LEDs indicate power on, satellite tracking, data logging, and event logging. The blue button on the left is the Power ON/OFF button.

Rear Panel

The µZ CGRS is provided with dual power ports, four RS-232 ports, and an external frequency reference port (figure 2). The µZ CGRS is 100% backward compatible with existing Z-12 CGRS cables.

External Frequency

Some applications require a clock more accurate than the internal oscillator. For this reason, the µZ-CGRS receiver has an External Frequency Reference input on the back panel. When the External Frequency mode is turned on, the internal clock is phase locked to the external reference, so that the receiver is in effect running off of the external reference.

External frequencies supported are 5 MHz, 10 MHz and 20 MHz. If no external frequency source is connected, the receiver will use the internal oscillator. When in external frequency mode, the receiver is monitoring the lock status of the phase-lock loop between the internal and external clocks as well as the presence of an

Figure 2. µZ-CGRS Rear Panel

external reference signal. If the receiver-switching mode is set to automatic, the receiver will automatically switch back to internal clock if the lock is lost, or no signal is detected for more than 25 sec.

Meteorological and Tilt Information

The firmware is capable of interfacing with external measurement devices such as the Paroscientific or Vaisala Meteorological Measurement Systems and the Applied Geomechanics geodetic Tiltmeters. This allows the receiver to get data from various sensors and send them to a control station and to a file onboard the receiver. Simultaneously, it records this information into the receiver's external memory.

Modem support

The µZ CGRS has improved modem support. The receiver supports the Z-modem protocol for more reliable data transfer than the typical X-modem protocol. In addition, one of the serial ports has been wired with all of the lines necessary for complete modem control (TXD, RXD, RTS, CTS, DSR, DTR, and DCD) rather than the minimum TXD and RXD lines found in may receivers. This makes the µZ CGRS ideal for remote, unattended operations.

Power Requirements

The µZ-CGRS including the antenna requires less than 7 Watts to operate. There are dual power ports on the back panel allowing multiple power sources. Accessory options allow the unit to automatically switch from AC to DC power in the event of AC power failure, and to switch back when AC power is restored. The receiver will start and operate normally with only 9VDC making it ideal for solar-powered installations.

Configurations

The following diagrams illustrate some of the possible configurations of the μZ-CGRS.

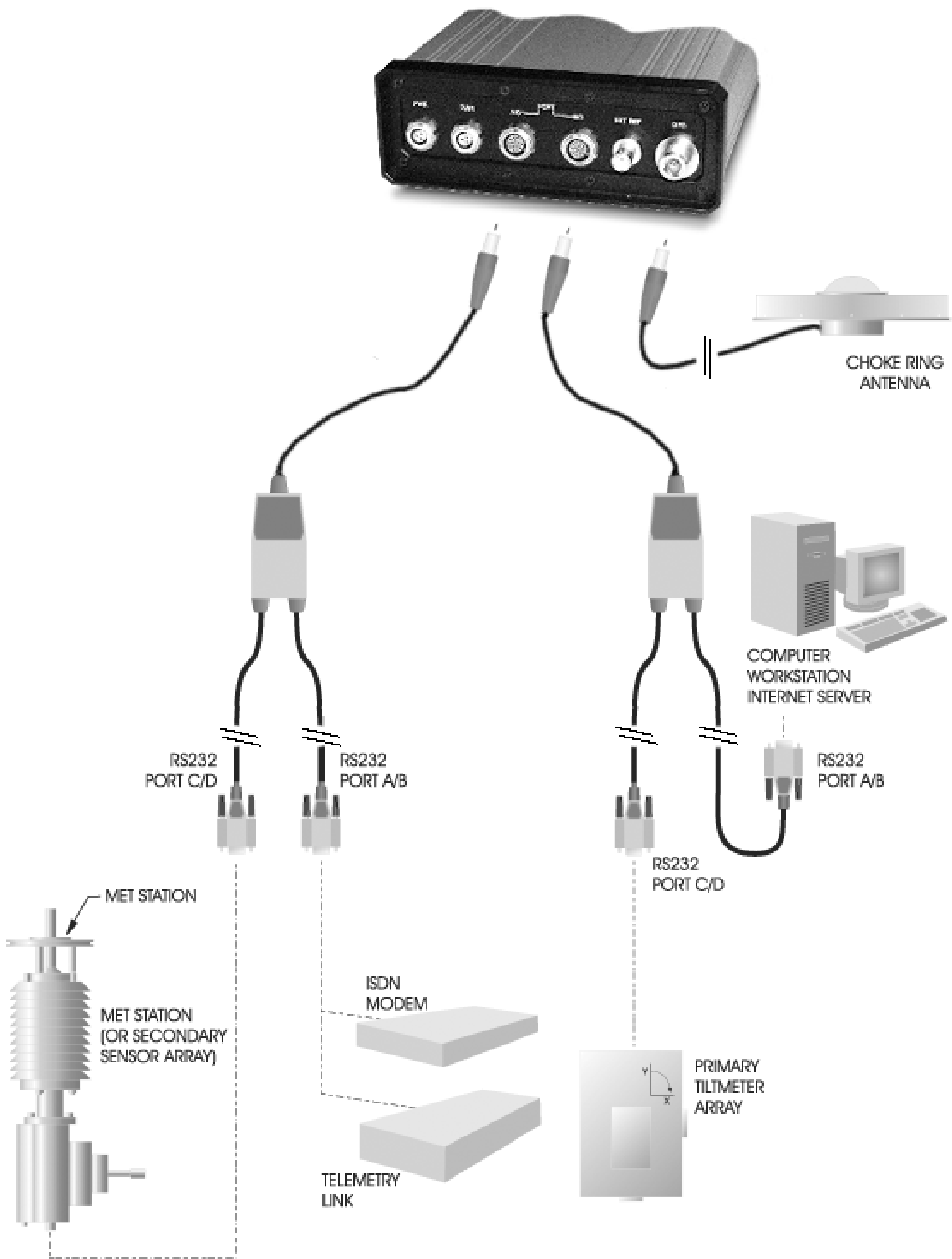

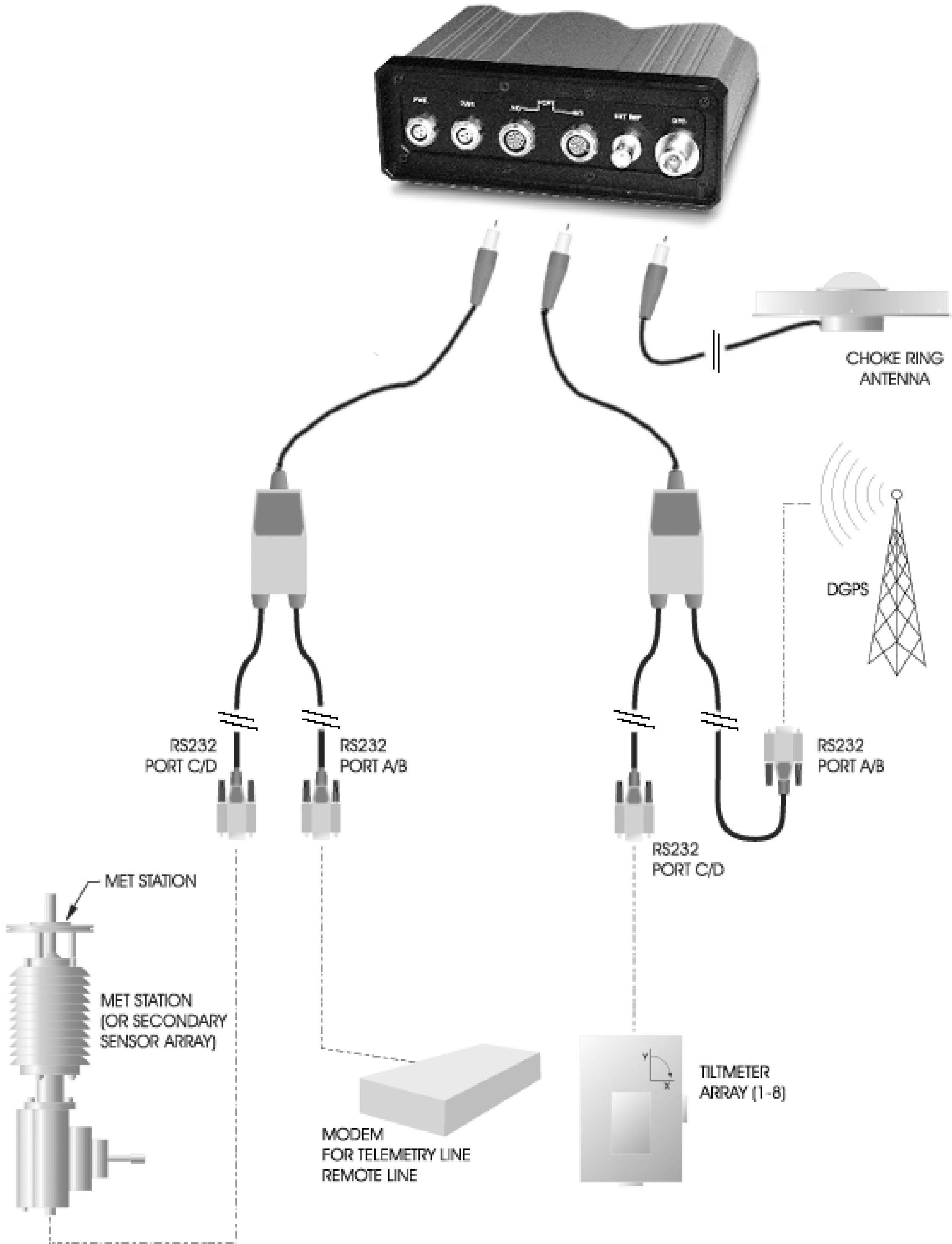
CHOKE RING ANTENNA
DGPS
RS232 PORT C/D
RS232 PORT A/B
RS232 PORT A/B
RS232 PORT C/D
MET STATION
MET STATION (OR SECONDARY SENSOR ARRAY)
MODEM FOR TELEMETRY LINE REMOTE LINE
TILTMETER ARRAY (1-8)

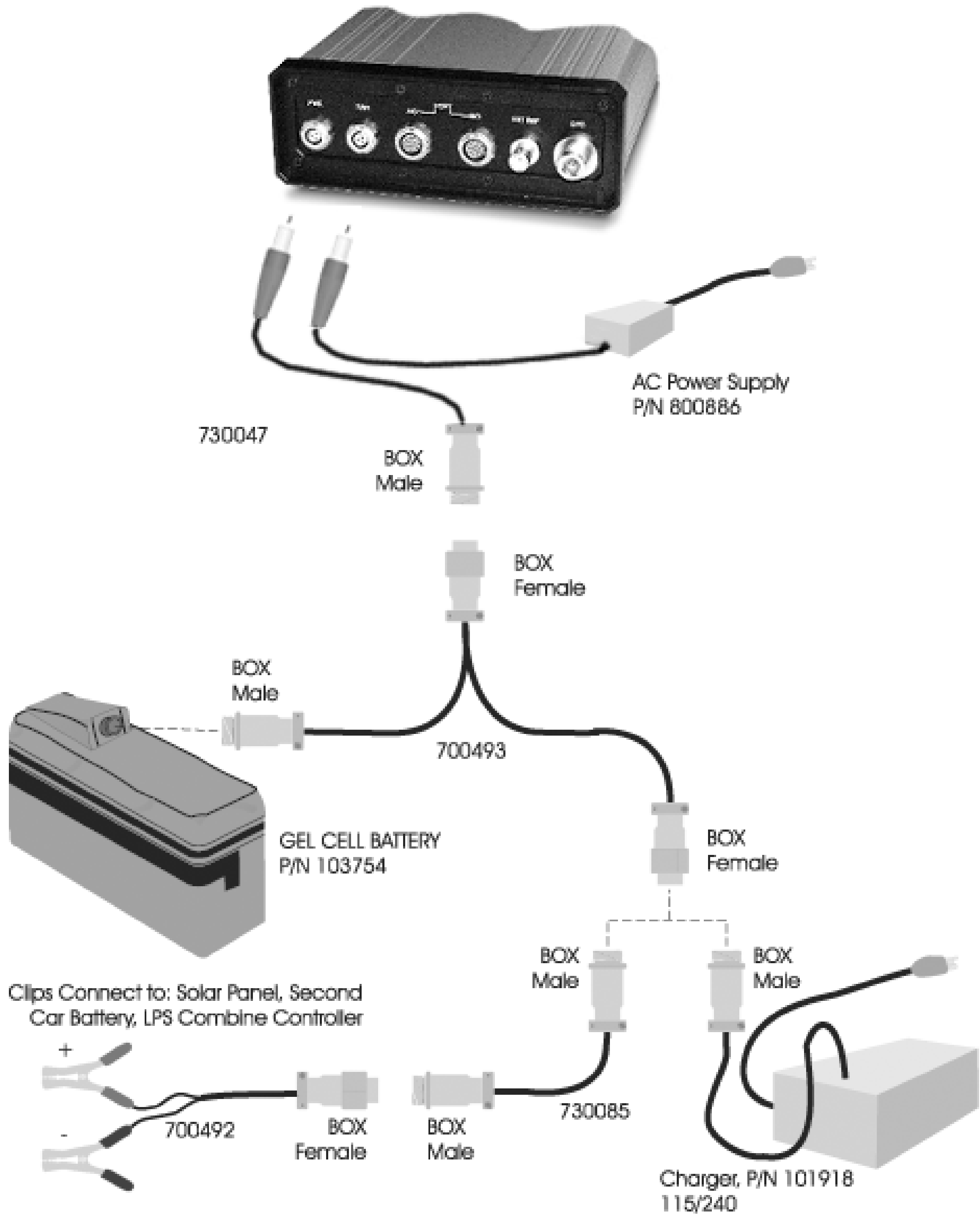

3. APPLICATIONS

The µZ CGRS is ideal for studies of crustal deformation, atmospheric monitoring, volcano monitoring, and structure deformation monitoring. The receiver will also operate as a differential base station outputting corrections for both pseudorange and carrier phase positioning for use in land survey, seismic survey, hydrographic survey, and precise navigation. The low power and robust modem support allow the system to be operated remotely on solar and battery power using radio modems to return the data.

The optional Geodetic Base Station Software on a co-located PC can log separate files of single-frequency and dual-frequency data from one receiver, as well as data at different sample rates. This allows the user to provide different data for different users from one receiver. For example, the user could create single-frequency files at 1-second interval for GIS users and dual-frequency data at 30-second interval for geodesy.

4. UNAVCO SUOMINET REPORT (Jackson et al, 2000)

UNAVCO is a consortium of over 100 international universities and laboratories joined to promote the use of the Global Positioning System (GPS) for high-accuracy geosciences research, which ranges from plate kinematics, earthquake processes and volcanoes, to sea level change and the atmosphere. UNAVCO supports both university-based activities and a central Facility that provide GPS technology capability to the broad GPS user community and specific project support to investigators funded by the National Science Foundation (NSF) and National Aeronautics and Space Administration (NASA).

UNAVCO was asked by its community to provide comprehensive GPS receiver testing report and three GPS manufacturers, Magellan Corporation's Ashtech Precision Products, Trimble Navigation, and Javad Positioning Systems, voluntarily submitted to this testing using their latest high-precision products. The test started in October 1999 and finished in May 2000. The field data collection lasted from 12 January to 8 March. The testing procedure was based on the procedure in UNAVCO Academic Research Infrastructure (ARI) Receiver and Antenna Test Report (Rocken et al, 1996). The final report (http://www.unavco.ucar.edu/dev_test/publications/suominetreportv_4.pdf) has 59 pages with 54 figures and 28 tables. The carrier phase measurement accuracy and carrier phase tracking performance have been extensively tested and compared in the report.

Carrier Phase Measurement Accuracy

The carrier phase measurement accuracy has been assessed through zero-baseline testing and short-baseline testing. Zero-baseline testing is used to assess the accuracy of raw carrier phase measurements. The root mean squares of raw carrier phase measurements can be estimated by scaling the root mean squares of double-differenced carrier phase measurements over a zero baseline by a factor of 0.5. Zero-baseline tests use two receivers connected to the same antenna where all common errors due to multipath and propagation effects are canceled. Therefore the raw measurement RMS reflects the measurement noise level, rather than the systematic errors, e.g. multipath, atmosphere delay, etc. The UNAVCO testing results are listed in the row "Raw Measurement RMS" in Table 1 for L1, L2 and ionosphere-free combination (L3) carrier phase measurements based on the results of Tables 4-1, 4-2 and 4-3 in the UNAVCO report. The raw measurement noise level can also be seen through the zero-baseline double-difference residuals, shown in Figure 3.

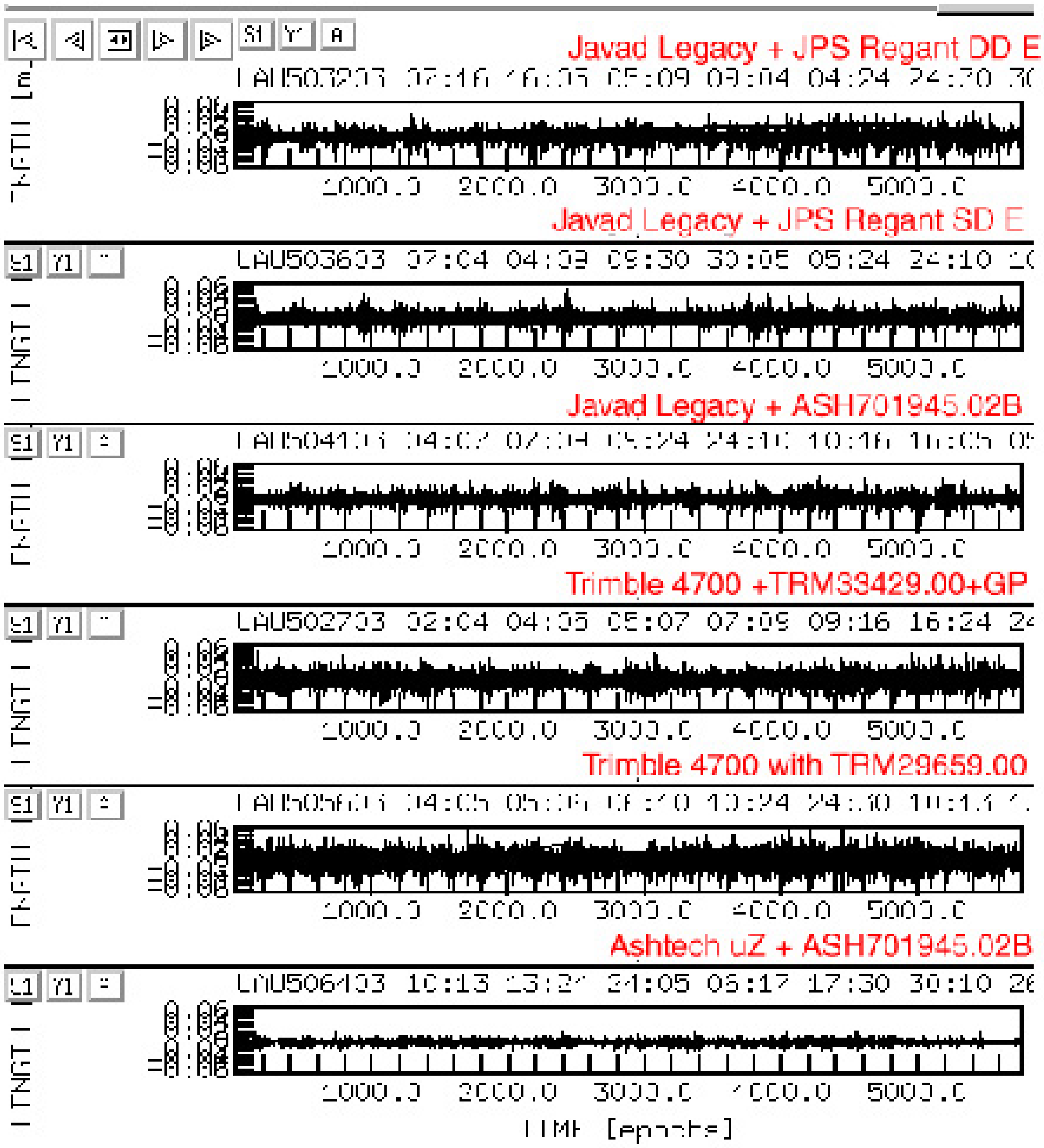
Javad Legacy + JPS Regant DD E
Javad Legacy + JPS Regant SD E
Javad Legacy + ASH701945.02B
Trimble 4700 +TRM33429.00+GP
Trimble 4700 with TRM29659.00
Ashtech uZ + ASH701945.02B

Figure 3a

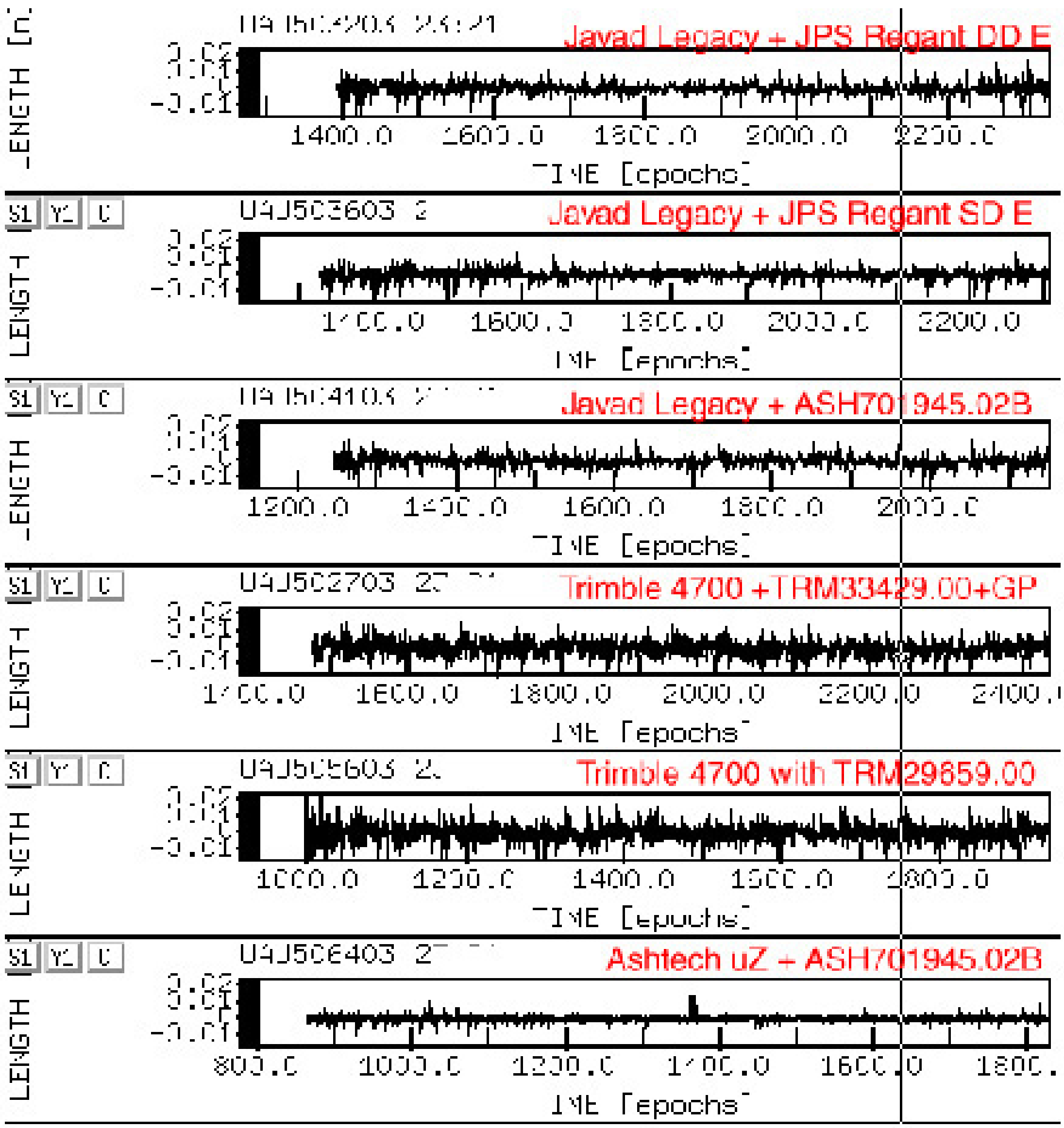

Figure 3b

Figure 3: Figure 3a is a plot of L3 zero baseline double-difference residuals for all satellites which appeared in Figure 4-10 in the original UNAVCO report. Scale is 6 to -6 cm. Figure 3b is a plot of L3 zero baseline double-difference residuals for satellites 23 and 21 which appeared in Figure 4-11 in the original UNAVCO report. Scale is 2 to -1 cm. Traces are, from top to bottom Javad Legacy with JPS Regant DD E, Javad Legacy with JPS Regant SD E, Javad Legacy with ASH701945.02B, Trimble 4700 with TRM33429.00+GP, Trimble 4700 with TRM29659.00, and Ashtech µZ with ASH701945.02B.

The repeatability of the short baseline solutions and double-differenced residual plots show the carrier phase measurement noise level, hardware delay, multipath reduction ability, etc. The RMS values showing the baseline repeatability for different receivers are listed in Table 1. The double differenced residuals are plotted in Figure 4.

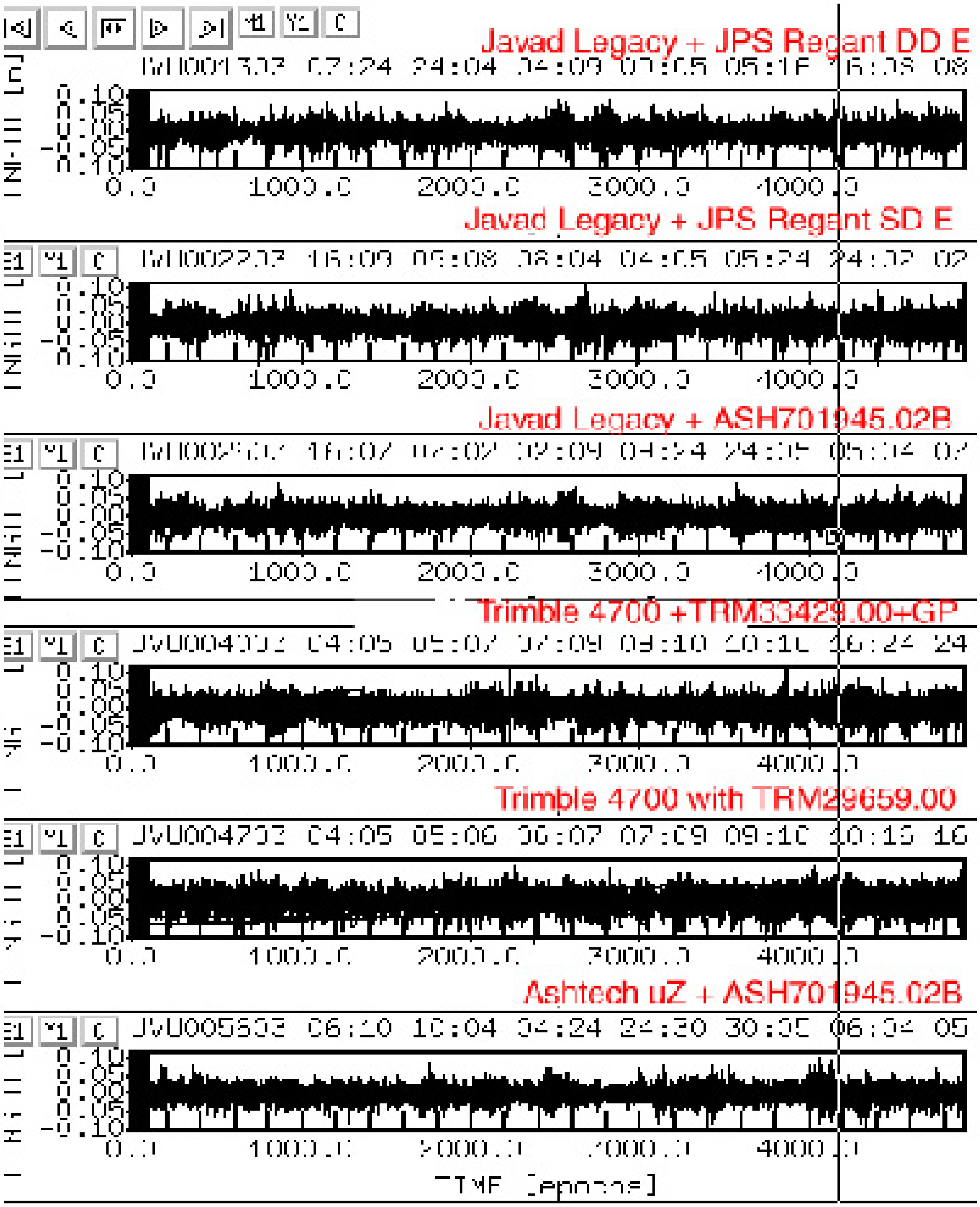
Javad Legacy + JPS Regant DD E
Javad Legacy + JPS Regant SD E
Javad Legacy + ASH701945.02B
Trimble 4700 +TRM33429.00+GP
Trimble 4700 with TRM29659.00
Ashtech uZ + ASH701945.02B

Figure 4a

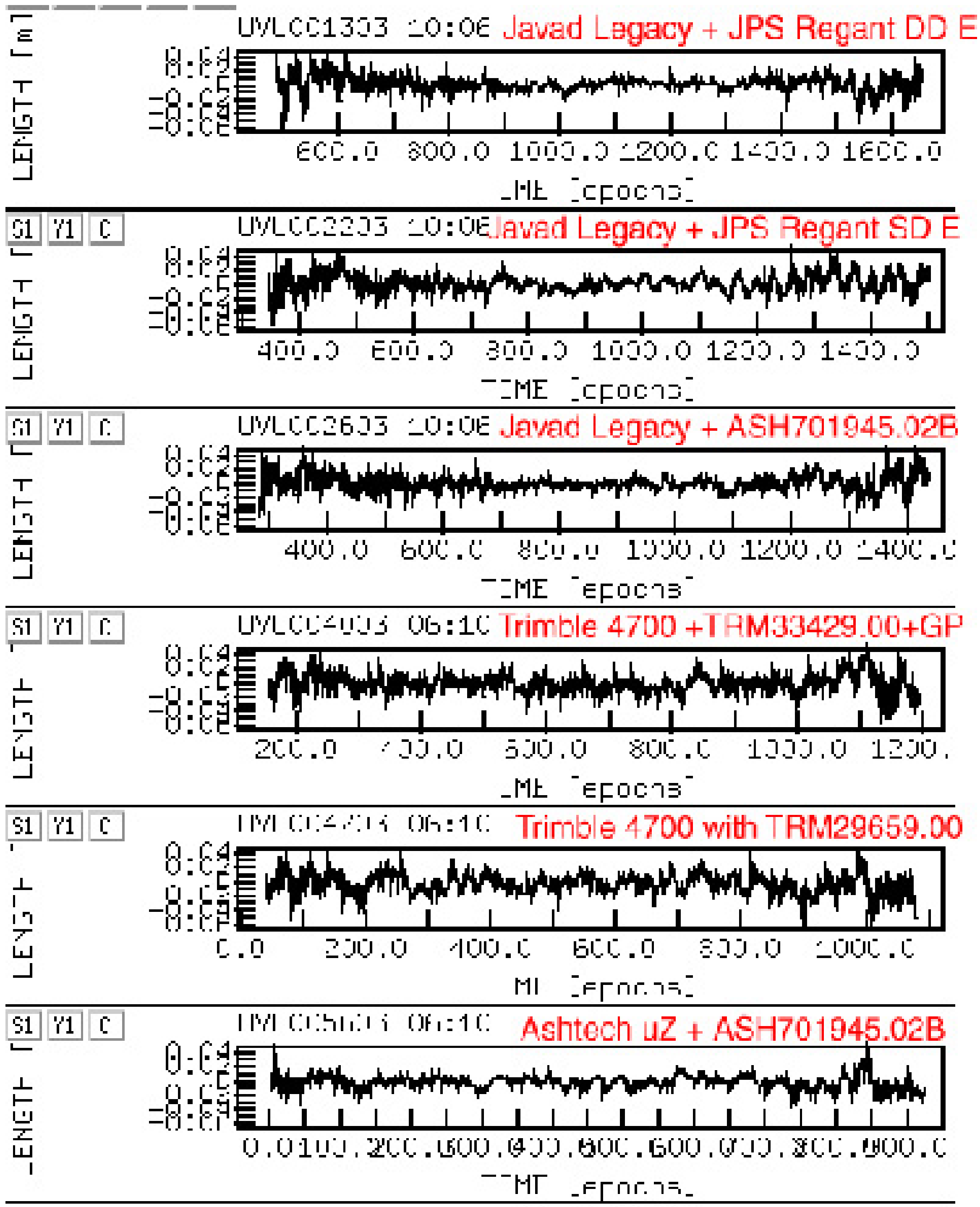

Figure 4b

Figure 4: Figure 4a is the double-difference residual plots for all satellites for short baseline L3 solutions (Figure 5-11 in the original report). Scale is 10 to -10 cm. Figure 4b is the double-difference residual plots for short baseline L3 solutions showing SV 10-6 pair (Figure 5-12 in the original report). Scale is 4 to -6 cm. Traces are, from top to bottom Javad Legacy with JPS Regant DD E, Javad Legacy with JPS Regant SD E, Javad Legacy with ASH701945.02B, Trimble 4700 with TRM33429.00+GP, Trimble 4700 with TRM29659.00, and Ashtech µZ with ASH701945.02B.

In addition, the troposphere delay has also been estimated to assess the accuracy of the carrier phase measurements. The difference of the troposphere delays at two receivers should be zero for zero baseline because both receivers are connected to the same antenna, and close to zero for short-baselines because the troposphere delays are similar. The troposphere delay estimations over zero or short baselines show the errors in the carrier phase measurement. The smaller the estimated values of the troposphere delay, the higher the quality of the raw carrier phase measurement. The hourly solutions using ionosphere-free combination (L3) are plotted in Figure 5. Troposphere delay estimations over short baselines reflect the similar information, which are listed in Row "Short-Baseline Troposphere" in Table 1.

It can be seen that Ashtech μZ-CGRS has overall best performance in terms of carrier phase measurement accuracy.

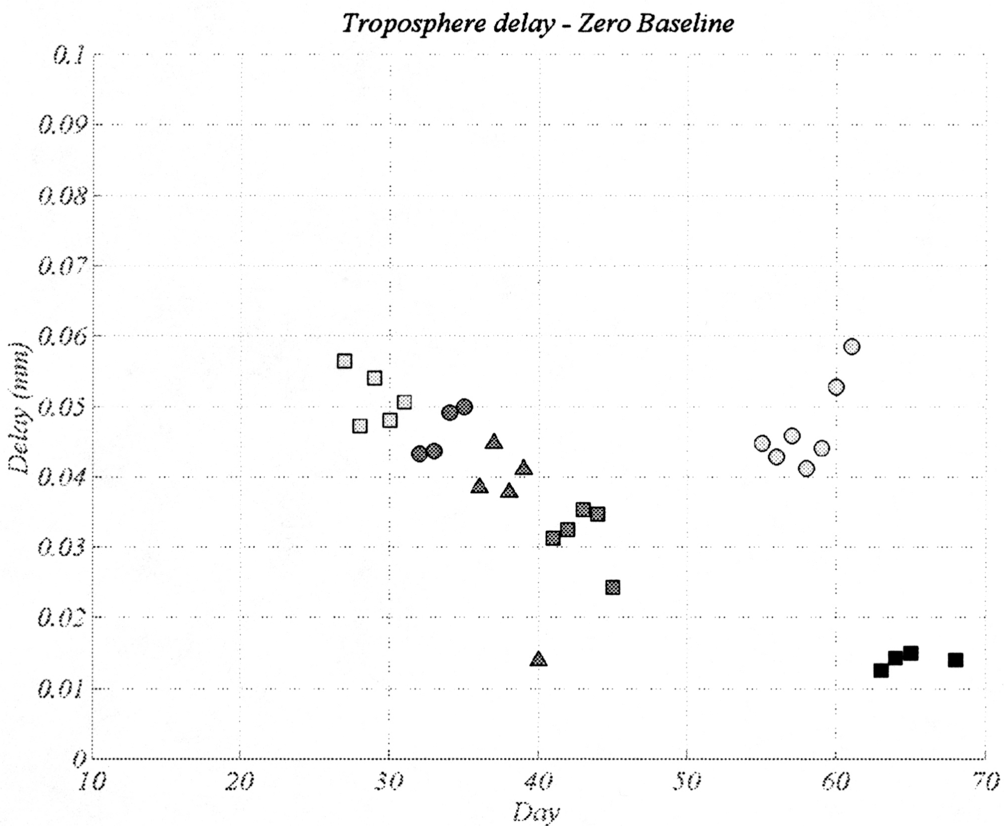

Figure 5: Residual Troposphere delay based on L3 zero-baseline solutions (Figure 4-12 in UNAVCO report). ■ Ashtech μZ with Ash701945.02B Ashtech Choke Ring Antenna; ▩ Javad Legacy with Ash701945.02B Choke Ring Antenna; ● Javad Legacy with JPS Regant DD E Choke Ring Antenna; ▲ Javad Legacy with JPS Regant SD E Choke Ring Antenna; □ Trimble 4700 with TRM33429.00 + GP Trimble Microcentered Antenna; and ○ Trimble 4700 with TRM29659.00 Trimble Choke Ring Antenna.

Table 1. Summary of Accuracy Performance for Carrier Phase Measurements Based on UNAVCO Report

	Freq.	ASH μZ	JPS AshA	JPS DD	JPS SD	TRMB GP	TRMB CR	References in the report
Raw Measurement RMS (mm)	L1	0.3	0.8	1.1	0.9	0.9	1.0	Tab. 4-1
	L2	0.5	1.1	2.4	1.3	1.7	2.2	Tab. 4-2
	L3	0.7	1.5	3.4	1.8	2.7	3.6	Tab. 4-3
Short-Baseline Repeatability RMS (mm)	L1	0.14	0.10	1.00	0.37	0.24	0.30	Tab. 5-1
	L2	0.24	0.57	0.71	0.55	0.17	0.24	Tab. 5-2
	L3	0.24	0.95	1.81	0.75	0.54	0.65	Tab. 5-3
Short-Baseline Troposphere (mm)	L3	0.63	0.62	0.86	0.78	0.81	0.92	Tab. 5-4

Carrier Phase Tracking Performance

The carrier phase tracking performance is summarized in Table 2. The cycle slip percentages are determined by (1) using the root-mean square of the linear combinations of the pseudorange and carrier phase measurements, which is affected by pseudorange measurement noise; and, (2) using time derivative of the ionosphere delay, which is not affected by pseudorange measurement noise (Estey & Meertens, 1999). Therefore the cycle slip percentages may also include big noise from pseudorange measurements. The results are shown in the first row of the Table 2. If only the pseudoranges on L1 or L2 are used, the cycle slip percentages detected are listed in the second or third row, respectively. The ratio values of the number of observations and the number of cycle slips are listed in the fourth row. The cycle slip percentages detected by the time derivative of ionosphere delay (IOD) are listed the fifth row. The last column gives the table number in the UNAVCO report from which the data were extracted.

Ashtech μZ-CGRS and Trimble 4700 with both antennas show the highest performance at elevation angle down to 5 degrees. Trimble 4700 with Microcentered antenna shows slightly better performance from 0 degree to 5 degrees than Ashtech μZ-CGRS and Trimble 4700 with Trimble choke ring antenna. JPS receivers show the worst results on the carrier phase tracking, especially at elevations from 0 degree to 10 degrees.

Table 2. Summary of Carrier Phase Tracking Performance Based on UNAVCO Report

	Elev degrees	ASH μZ (s)	ASH μZ (u)	JPS AshA	JPS DD	JPS SD	TRMB GP	TRMB CR	Ref. Tables
Cycle slip (CS) Percentages	90-10	0.01	0.01	0.01	0.09	0.05	0.01	0.00	3-1
	10-5	0.03	0.04	0.44	2.88	1.83	0.01	0.04	3-2
	5-0	0.19	0.21	2.70	8.55	4.26	0.02	0.12	3-3
CS percentages using P1 only	10-5	0.07	0.35	0.39	2.10	1.35	0.01	0.02	3-6
	5-0	0.19	0.83	2.80	5.42	2.96	0.31	0.13	3-8
CS percentages using P2 only	10-5	0.06	0.21	3.18	2.38	4.98	0.01	0.01	3-7
	5-0	0.19	0.65	5.85	6.84	5.64	0.13	0.02	3-9
Observations per slips[2]		22198	21587	17386	1120	2887	31907	20973	3-10
IOD	10-5	0.02	0.02	0.40	2.76	1.60	0.01	0.01	3-11
	5-0	0.03	0.03	2.43	7.52	3.19	0.10	0.01	3-12

Note that Column 3 gives the results from smoothed pseudorange measurements from the Ashtech μZ-CGRS receiver, and Column 4 is based on raw pseudorange measurements for the same receiver. The Ashtech μZ-CGRS receiver is designed to support geodetic data collection and to broadcast differential corrections for both code and carrier phase RTK operations. The reference station community often requires both the "raw" and the carrier-phase-smoothed pseudorange measurements to be available in real-time. Therefore, the Ashtech μZ-CGRS has been designed to provide *both* raw and carrier-phase-smoothed pseudoranges for *both* post-mission and real-time operations. The μZ CGRS carrier-phase-smoothed pseudoranges are generated in real time using smoothing parameters that are derived from the receiver's carrier phase measurements. The smoothing of the pseudoranges does not affect the independence of each epoch's carrier phase data.

It should be noted that GPS manufacturers typically do not output their raw sampled data as "raw" pseudorange unless it is at a very high rate such as 50 Hz. Some type of integration is applied to the individually sampled measurements to create the output. Increasing the integration time lowers the noise by the square root of the number of measurements integrated. Therefore one-second data may be more or less noisy depending on the native sampling rate of the GPS chip and the integration algorithm used to create the one-second point from the raw sampled data.

References

Estey, L., & Meertens, C., (1999). TEQC: The multipurpose toolkit for GPS/GLONASS data. GPS Solutions Vol. 3, No. 1 pp. 44-49.

Rocken, C., Meertens, C., Stephens, B., Braun, J., Van Hove, T., Perry, S., Ruud, O., McCallum, M., & Richardson, J., (1996). UNAVCO Academic Research Infrastructure (ARI) Receiver and Antenna Test Report. UNAVCO Boulder Facility Internal Report.

Jackson, M., Meertens, C., Andreatta, V., & Van Hove, T., (2000). GPS Receiver and Antenna Testing Report for SuomiNet, University NAVSTAR Consortium, Boulder CO, http://www.unavco.ucar.edu/dev_test/publications/suominetreportv_4.pdf